2:1 Dioctahedral Smectites as a Selective Sorbent for Dioxins and Furans: Reactivity Index Study

Abhijit Chatterjee,* Takashi Iwasaki, and Takeo Ebina

Environmental Functional Material Group, National Institute of Advanced Industrial Science and Technology, AIST Tohoku, 4-2-1 Nigatake, Miyagino-ku, Sendai 983-8551, Japan

Received: July 16, 2001; In Final Form: October 23, 2001

A suitable sorbent from the dioctahedral smectite family for the sorption of 2,3,7,8-terachlorinated/brominated dibenzo-*p*-dioxins (TCDD,TBDD), tetrachlorinated/brominated dibenzo furans (TCDF, TBDF) is investigated by means of a range of reactivity index using density functional theory (DFT). From the values of the local softness and the charge on the hydrogen atom of the bridging/structural (occurring on the surface) hydroxyl attached to the octahedral/tetrahedral metal site present in smectite, used as first approximation to the local hardness, it is concluded that the local acidities of the inorganic material systems are dependent on several characteristics that are of importance within the framework of the hard and soft acids and bases (HSAB) principle. We first aimed to rationalize an understanding to locate the active site of dioxins and furans by the local softness calculation. We compared its activity with that of the OH group of both octahedrally and terahedrally substituted members of the dioctahedral smectite family. We compared the probability of surface hydrogen bonding with that which resulted from the interaction of bridging hydroxyl present at the octahedral site in clays. By the interaction between systems, we validate the proposition for designing a novel qualitative way to choose the best sorption material both in terms of isomorphous substitution of clays and the nature of the interacting molecule.

Introduction

Polychlorinated/polybrominated dibenzo-*p*-dioxins/furans (PCDDs, PBDDs, PCDFs, PBDFs), which are highly toxic materials, have been detected as trace contaminants in municipal incinerators[1] and industrial heating facilities during combustion.[2] Recently a global poisoning fear has been generated due to release of these substances in the environment.[2,3] This has triggered a large number of experimental and theoretical studies[4−6] aimed to elucidate the chemical and biological properties of these compounds. PCDDs are the most widely studied variety. There has been significant, although lesser, interest in the formation of PBDDs from the combustion of brominated flame redundant of various compositions.[7,8] Experimental information about the molecular parameters of dioxin/furans is hard to obtain due to its high toxicity. Molecular orbital calculations can provide vital information about these molecules.

There are many empirical and ab initio theoretical studies on PCDD.[9−13] The mechanism of the toxicity attributed to the PCDDs depends on structurally related properties.[11] Fuji et al.[12] have studied the structure and energy of TCDD using the Gaussian 92 program at two ab initio molecular orbital levels: RHF/6-31G and RHF/6-31G*. The results are comparable with the structural information obtained from X-ray diffraction study. They did not talk about the active site of the TCDD. Now, to destroy dioxin by biological, chemical, or thermal means involves high costs, because it occurs in such low concentrations in the environment. Due to its high toxicity, there is no lower limit at which dioxin can be considered safe and would therefore require no remedial action. The desired concentration (i.e., threshold value for estimation) can be achieved through adsorption of the dioxin from solution onto a solid.[13] The optimal solid sorbent for dioxin should have the following properties: low cost, ease of handling, environmental neutrality, high affinity, high selectivity, and the capability of being integrated into a dioxin-destruction process. Among many candidates examined experimentally, clays meet the majority of the above criteria; however, clays in their natural state exhibit neither high affinity for nor removal selectivity of hydrophobic compounds such as dioxin.[14,15] An inorganic clay (hydroxy-Al-Montmorillonite) and an organoclay (humic acid-hydroxy-Al-Montmorillonite) were developed.[16,17] The high bonding affinity of the former for dioxin was attributed to the clay's ability to function as a two-dimensional zeolite. Boyd et al.[18] have shown that Cu^{2+}-exchanged smectite catalyzes dioxin dechlorination reactions.

Montmorillonite and Beidellite are members of the 2:1 dioctahedral smectite family, which share the common feature that two octahedral sites sandwich a sheet of octahedrally coordinated metal ion. Substitution of a bivalent metal ion for octahedral aluminum in montmorillonite and substitution of a trivalent metal ion for tetrahedral silicon in Beidellite results in a net negative charge and an interaction with positive ions (exchangeable cation) to form a interlayer hydrated phase. Their activity lies in the layer charge that resulted either by octahedral substitution or by tetrahedral substitution. In any case, the hydroxyl hydrogen attached with octahedral metal ion through oxygen bridge or the structural hydroxyl occurring due to the substitution of tetrahedral ion act as the active site of clay for catalytic activity.[19] Now, we wish to compare the selectivity of the clays for sorption of dioxin and furan as well as the chloro and bromo variety. Even with the clays, we modulated the octahedral cation by isomorphous substitution with various

* Corresponding author. E-mail: c-abhijit@aist.go.jp. Phone: +81-22-237-5211. Fax: +81-22-237-5217.

10.1021/jp0127418 CCC: $22.00
Published on Web 01/08/2002

cations (Mg^{2+}, Fe^{2+}, Fe^{3+}, Li^{+}) and the results were compared with that of a clay variety where the layer charge occurs from tetrahedral substitution as mentioned in our earlier study.[19]

The hard soft acid−base (HSAB) principles classify the interaction between acids and bases in terms of global softness. Pearson proposed the global HSAB principle.[20] The global hardness was defined as the second derivative of energy with respect to the number of electrons at constant temperature and external potential, which includes the nuclear field. The global softness is the inverse of this. Pearson also suggested a principle of maximum hardness (PMH),[21] which states that, for a constant external potential, the system with the maximum global hardness is most stable. Recently, DFT has gained widespread use in quantum chemistry. Some DFT-based local properties, e.g., Fukui functions and local softness,[22] have already been used for reliable predictions in various types of electrophilic and nucleophilic reactions.[23−26] In our recent study[27] we proposed a reactivity index scale for heteroatomic interaction with zeolite framework. Moreover, Gazquez and Mendez[28] proposed that when two molecules A and B of equal softness interact, thereby implicitly assuming one of the species as nucleophile and the other as an electrophile, then a novel bond would likely form between an atom A and an atom B whose Fukui function values are close to each other.

The aim of the current study is to find a suitable sorbent from the smectite family for the sorption of dioxins and furans. Two types of hydroxyl hydrogen present in smectite in terms of tetrahedral and octahedral substitution are monitored. The location of hydroxyl hydrogen influences the activity of clay. The local reactivity index calculation is employed to find the perfect match between the interacting organic toxic pollutant and smectite members. Isomorphous substitution of octahedral metal present in montmorillonite type clays is monitored and compared with the Beidellite variety of clay for which the layer charge results from tetrahedral substitution. A reactivity index scale is proposed in terms of activity of clay materials chosen. A quantitative scale is also proposed for the selective sorption of the organic toxic molecules over the best performing clay material.

Theory

Let us first recall the definition of various quantities employed. The Fukui function $f(r)$ is defined by[22]

$$f(r) = [\delta\mu/\mathrm{d}v(r)]_N = [\delta\rho(r)/\delta N]_v \quad (1)$$

The function 'f' is thus a local quantity that has different values at different points in the species, N is the total number of electrons, μ is the chemical potential, and v is the potential acting on an electron due to all nuclei present. Since $\rho(r)$ as a function of N has slope discontinuities, eq 1 provides the following three reaction indices:[22]

$$f^{-}(r) = [\delta\rho(r)/\delta N]_v^{-} \text{ (governing electrophilic attack)}$$

$$f^{+}(r) = [\delta\rho(r)/\delta N]_v^{+} \text{ (governing nucleophilic attack)}$$

$$f^{0}(r) = {}^1/_2[f^{+}(r) + f^{-}(r)] \text{ (for radial attack)}$$

In a finite difference approximation, the condensed Fukui function[29] of an atom, say x, in a molecule with N electrons is defined as

$$f_x^{+} = [q_x(N+1) - q_x(N)] \text{ (for nucleophilic attack)}$$

$$f_x^{-} = [q_x(N) - q_x(N-1)] \text{ (for electrophilic attack)}$$

$$f_x^{0} = [q_x(N+1) - q_x(N-1)]/2 \text{ (for radical attack)} \quad (2)$$

where q_x is the electronic population of atom x in a molecule. In density functional theory, hardness (η) is defined as[30]

$$\eta = {}^1/_2(\delta^2 E/\delta N^2)v(r) = {}^1/_2\,(\delta\mu/\mathrm{d}N)_v$$

The global softness, S, is defined as the inverse of the global hardness, η.

$$S = 1/2\eta = (\delta N/\delta\mu)_v$$

The local softness $s(r)$ can be defined as

$$s(r) = (\delta\rho(r)/\delta\mu)_v \quad (3)$$

Equation 3 can also be written as

$$s(r) = [\delta\rho(r)/\delta N]v[\delta N/\delta\mu]_v = f(r)S \quad (4)$$

Thus, local softness contains the same information as the Fukui function $f(r)$ plus additional information about the total molecular softness, which is related to the global reactivity with respect to a reaction partner, as stated in the HSAB principle. Using the finite difference approximation, S can be approximated as

$$S = 1/(\mathrm{IE} - \mathrm{EA}) \quad (5)$$

where IE and EA are the first ionization energy and electron affinity of the molecule, respectively. Atomic softness values can easily be calculated by using eq 4, namely,

$$s_x^{+} = [q_x(N+1) - q_x(N)]S$$

$$s_x^{-} = [q_x(N) - q_x(N-1)]S$$

$$s_x^{0} = S[q_x(N+1) - q_x(N-1)]/2 \quad (6)$$

Computational Methodology and Model

In the present study, all calculations have been carried out with DFT[31] using the DMOL code of MSI Inc. A gradient corrected functional BLYP[32,33] and a DNP basis set[34] were used throughout the calculation. BLYP has already shown its credibility for explaining weak hydrogen bond type interactions in comparison to MP2 level calculations.[35,36] It is also useful in describing the interaction of heteroatomic molecules with zeolite framework cluster.[27] Basis set superposition error (BSSE) was also calculated for the current basis set in nonlocal density approximation (NLDA) using the Boys−Bernardi method.[37] Geometries of the interacting 2,3,7,8-TCDD/TBDD/TCDF/TBDF along with the individual clay cluster models representing different isomorphous substitution in the octahedral aluminum/tetrahedral silicon of dioctahedral smectites were fully optimized for calculating the reactivity index. The theory for reactivity index calculations is mentioned elsewhere in detail.[27] Single-point calculations of the cation and anion of each molecule at the optimized geometry of the neutral molecule were also carried out to evaluate Fukui functions and global and local softness. The condensed Fukui function and atomic softness were evaluated using eqs 2 and 6, respectively. The gross atomic charges were evaluated by using the technique of electrostatic

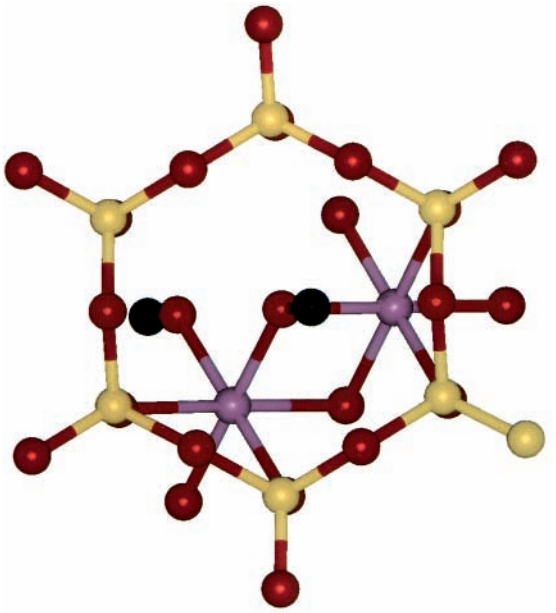

Figure 1. Cluster model of Montmorillonite with six tetrahedral silicons and two octahedral aluminums. It is the top view of the cluster. The color code is as follows: red (oxygen); yellow (silicon); violet (octahedral aluminum); black (hydrogen).

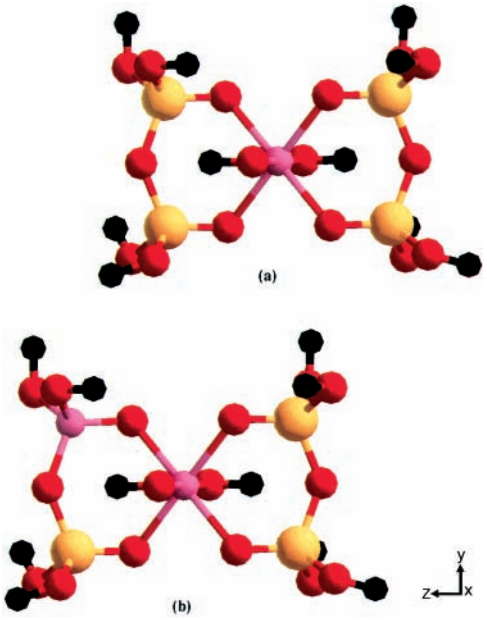

Figure 2. Initial configuration of clay cluster having the formula (a) $TSi_4O_{14}H_{10}$ (representing Montmorillonite) and (b) $AlSi_3AlO_{16}H_{11}$ (representing Beidellite) is shown. The color code is as follows: red (oxygen); yellow (silicon); violet (octahedral aluminum); black (hydrogen).

potential (ESP) driven charges. It is well-known that Mulliken charges are highly basis set dependent, whereas ESP driven charges show less basis set dependence[27,38,39] and are better descriptors of the molecular electronic density distribution.

The ideal formula of the clay montmorillonite, a member of the 2:1 dioctahedral smectite family, is $(Na^+_x, nH_2O)(Al_{4-x}Mg_x)Si_8O_{20}(OH)_4$.[40] The $Al_2Si_6O_{24}H_{18}$ cluster was generated from the clay structure as shown in Figure 1. Figure 1 displays the top view of one tetrahedral and one octahedral sheet, showing the hexagonal cavities at the oxygen surface of the silicon layers. The dangling bonds were saturated with hydrogens, not shown in Figure 1 for visual clarity. Two localized clusters were generated to represent two types of 2:1 dioctahedral smectite: (a) Montmorillonite and (b) Beidellite. The clusters have the formula $TSi_4O_{16}H_{10}$, where T = Fe^{3+}, Mg^{2+}, Fe^{2+}, Li^+; and $AlSi_3AlO_{16}H_{11}$, where the adjacent silicon and aluminum atoms occurring in the clay lattice are replaced by hydrogens to preserve the electroneutrality of the model. The clusters are shown in Figure 2a and b, respectively.

Results and Discussion

The aim of the current communication is to show the selectivity of dioxin and furan molecules toward dioctahedral smectite. The two most commonly available varieties of smectite are chosen with different location of layer charge, which is responsible for its activity. The sorption of available range of toxic dioxins and furans on the clay moiety were monitored to choose the best material. The electronic and structural properties of the dioxin and furan varieties along with the clay cluster models are first rationalized. The global softness values of the clay cluster models as well as the interacting molecules are calculated using DFT and are presented in Table 1. The values of nucleophilic condensed local softness (s_x^+) and condensed Fukui function (f_x^+) of the individual atoms of the clay cluster models obtained through the ESP technique at the DFT level are shown in Table 2. A comparison of the best variety of montmorillonite and aluminum substituted Beidellite variety is given in Table 3. The values of electrophilic condensed local softness (s_x^-) and condensed Fukui function (f_x^-) of the individual atoms of the TCDD/TBDD molecules obtained through the ESP technique at DFT level are shown in Table 4. The comparison of Fukui function and local softness values for furan molecules of both the chloro and bromo varieties is shown in Table 5. It is observed from Table 1 that those global softness values for the clay cluster models are lower than that of the interacting molecular species. So to test the HSAB principle, it seems to be important to analyze whether the local softness values, Fukui functions, or reactive indices for the constituent

TABLE 1: Global Softness Values (in au) for Clay Clusters and Substituted Dioxin and Furan Molecules

molecules	global softness (au)
$[LiSi_4O_{16}H_{10}]^{2-}$	1.86291
$[MgSi_4O_{16}H_{10}]^-$	1.52173
$[FeSi_4O_{16}H_{10}]^-$	1.46732
$[FeSi_4O_{16}H_{10}]$	1.28899
$AlSi_3AlO_{16}H_{11}$	2.22610
TCDD	4.08804
TBDD	3.98406
TCDF	3.01750
TBDF	3.14465

TABLE 2: Condensed Local Softness and Fukui Function Values (au) for Clay Clusters with Different Isomorphous Substitution by ESP Technique Using DFT

	substituent cation for octahedral Al^{3+}							
	Mg^{2+}		Fe^{3+}		Fe^{2+}		Li^+	
atoms	f_x^+	s_x^+	f_x^+	s_x^+	f_x^+	s_x^+	f_x^+	s_x^+
T1[a]	0.150	0.229	0.221	0.284	0.144	0.212	0.097	0.180
Si	0.058	0.089	0.093	0.120	0.049	0.073	0.040	0.074
Os[b]	0.061	0.093	0.106	0.136	0.059	0.087	0.041	0.076
Oh[c]	**0.402**	**0.612**	**0.275**	**0.354**	**0.325**	**0.478**	**0.124**	**0.231**
Oh	**0.458**	**0.698**	**0.348**	**0.448**	**0.370**	**0.543**	**0.149**	**0.277**
Hs[d]	0.016	0.025	0.015	0.019	0.012	0.018	0.010	0.018
Hh[e]	**0.323**	**0.492**	**0.335**	**0.432**	**0.314**	**0.462**	**0.211**	**0.393**
Hh	**0.396**	**0.603**	**0.428**	**0.551**	**0.400**	**0.587**	**0.233**	**0.434**

[a] T1 = substituent cation. [b] Os = structural oxygen. [c] Oh = hydroxyl oxygen. [d] Hs = structural hydrogen. [e] Hh = hydroxyl hydrogen.

TABLE 3: Comparison of Condensed Local Softness and Fukui Function Values (in au) for Clay Clusters Representing Montmorillonite (substituted cation for octahedral Al^{3+}) and Beidellite (substituted cation for tetrahedral Si^{4+})

	substituted cation for octahedral Al^{3+} and tetrahedral Si^{4+}			
	Mg^{2+} (for octahedral Al^{3+})		Al^{3+} (for tetrahedral Si^{4+})	
atoms	f_x^+	s_x^+	f_x^+	s_x^+
T1[a]	0.150	0.229	0.219	0.487
Si	0.058	0.089	0.090	0.200
Os[b]	0.061	0.093	0.234	0.520
Oh[c]	**0.402**	**0.612**	**0.170**	**0.378**
Oh	**0.458**	**0.698**	**0.187**	**0.416**
Hs[d]	0.016	0.025	0.302	0.672
Hh[e]	**0.323**	**0.492**	**0.168**	**0.373**
Hh	**0.396**	**0.603**	**0.172**	**0.382**

[a] T1 = substituent cation. [b] Os = structural oxygen. [c] Oh = hydroxyl oxygen. [d] Hs = structural hydrogen. [e] Hh = hydroxyl hydrogen.

TABLE 4: Condensed Local Softness and Fukui Function Values (in au) for TCDD and TBDD Using ESP Technique with DFT

	TCDD		TBDD	
atoms	f_x^-	s_x^-	f_x^-	s_x^-
C1	0.021	0.085	0.008	0.031
C2	0.021	0.085	0.009	0.035
C3	0.030	0.122	0.021	0.083
C4	0.024	0.098	0.021	0.083
C5	0.024	0.098	0.021	0.083
C6	0.030	0.122	0.021	0.083
O7	0.051	0.208	0.056	0.223
C8	0.024	0.098	0.021	0.083
C9	0.024	0.098	0.021	0.083
O10	0.052	0.212	0.056	0.223
C11	0.029	0.118	0.020	0.079
C12	0.022	0.089	0.009	0.035
C13	0.022	0.089	0.008	0.031
C14	0.030	0.122	0.021	0.083
Cl15	0.112	0.457	0.135	0.537
Cl16	0.111	0.453	0.135	0.537
H17	0.037	0.151	0.037	0.147
H18	0.037	0.151	0.037	0.147
H19	0.037	0.151	0.037	0.147
Cl20	0.111	0.453	0.135	0.537
Cl21	0.111	0.453	0.135	0.537
H22	0.037	0.151	0.037	0.147

atoms of the cluster models and interacting molecular species will be the more reliable parameter. To rationalize the phenomenon and to trace the selectivity of clays for the respective organic pollutants, first, a qualitative trend is proposed in terms of the local reactivity descriptors in the helm of HSAB between the different clay clusters and the interacting molecules. This order is validated by the interaction energy calculations. Now in the clay cluster, two different types of hydroxyl have been observed: (1) is the structural hydroxyl present during a tetrahedral substitution occurring in the Beidellite variety of clay and (2) hydroxyl hydrogen attached with octahedral metal cation present in Montmorillonite variety. The orientation of the optimized interacting molecular conformation is also monitored to justify its interaction with octahedral/tetrahedral metal ion present in the clay framework.

Activity of Isomorphously Substituted Clay Clusters in Terms of Reactivity Index. To choose the best sorbent material from the clay structures first we need to know the active center. For Montmorillonite, Li^+, Mg^{2+}, Fe^{2+}, and Fe^{3+} replaced the Al^{3+} ion present at the octahedral site. The tetrahedral Si^{4+} of Beidellite is replaced by Al^{3+} to monitor the role of tetrahedral substitution on the sorption of those organic molecules mentioned before. In each case the cluster was totally optimized. The initial configurations of the representative clusters are shown in Figure 2a and b, respectively. As we have seen earlier, there are two different alumina present in the dioctahedral smectites with different geometric parameters.[41] The order of substitution follows the order $Fe^{3+} > Mg^{2+} > Fe^{2+} > Li^+$. It is noted below that the magnitude of electron density (numbers in parentheses) transferred to the metal ion is Al^{3+} (2.56) > Fe^{3+} (2.09) > Mg^{2+} (1.52) > Fe^{2+} (1.28) > Li^+ (0.06). Thus, rather than the formal charges associated with the various cations, the calculated in situ net charges are given by 0.44+, 0.91+, 0.48+, 0.72+, and 0.94+, where the same cation order as in the above set of inequalities has been kept. This ordering agrees with the proposal of Goldschmidt.[42] His proposal was based on the approximate relative sizes of metal ions in their appropriate valences. The results partially are in agreement with the stability order proposed by Arnowitz et al. for isomorphous substitution in clays using the self-consistent charge extended Hückel program.[43] It is observed that insertion of Li^+ in place of Al^{3+} in the octahedral layer is the least favorable process. When these results are combined with that of the substitution energy resulting from the substitution of tetrahedral Si^{4+} by Al^{3+}, the order is as follows: $Al^{3+} > Fe^{3+} > Mg^{2+} > Fe^{2+} > Li^+$.

TABLE 5: Condensed Local Softness and Fukui Function Values (in au) for TCDF and TBDF Using ESP Technique with DFT

	TCDF		TBDF	
atoms	f_x^-	s_x^-	f_x^-	s_x^-
C1	0.053	0.159	0.039	0.122
C2	−0.001	−0.003	−0.004	−0.012
C3	0.042	0.126	0.042	0.132
C4	−0.003	−0.009	−0.009	−0.028
C5	0.005	0.015	0.012	0.037
C6	−0.036	−0.108	−0.021	−0.066
H7	0.036	0.108	0.036	0.113
H8	0.039	0.117	0.038	0.119
C9	−0.001	−0.003	−0.004	−0.012
C10	0.053	0.159	0.039	0.122
C11	−0.036	−0.108	−0.021	−0.066
C12	0.005	0.015	0.012	0.037
C13	−0.003	−0.009	−0.009	−0.028
C14	0.042	0.126	0.042	0.132
H15	0.036	0.108	0.036	0.113
H16	0.039	0.117	0.038	0.119
O17	0.044	0.132	0.041	0.128
Cl18	0.194	0.585	0.203	0.638
Cl19	0.148	0.446	0.144	0.452
Cl20	0.148	0.446	0.144	0.452
Cl21	0.194	0.585	0.203	0.638

As we have mentioned in our earlier paper,[41] the orientation of hydroxyl hydrogen attached to the octahedral aluminum or the isomorphously substituted cation plays a crucial role in its acidity and activity. Hence, we calculated the global and local reactivity parameters for the constituent atoms of the clay clusters. The global softness values are shown in Table 1. The global softness for the aluminum-substituted cluster representing Beidellite has the highest value, whereas the cluster with Fe^{2+} substitution has the lowest value. The order of the numbers is $Al^{3+} > Li^+ > Mg^{2+} > Fe^{2+} > Fe^{3+}$. To monitor the localized properties, the Fukui function (f_x^+) and local atomic softness (s_x^+) for the constituent atoms of the isomorphously substituted clusters representing Montmorillonite are calculated by ESP charges obtained from DFT, and the results are tabulated in Table 2. The results show that the activity order is different from that of the order predicted by the substitution energy. The substitution energy results predicted that Fe^{3+} substitution incurs the most stability in the case of Montmorillonite and Al^{3+} in

general. But when we try to monitor the activity of the hydroxyl group attached to the octahedral cation we get a different scenario. In a situation with Mg^{2+} as the isomorphous substituent, the hydroxyl hydrogen shows the most nucleophilicity, as shown in Table 2. In terms of the activity of the hydroxyl group, the order stands $Mg^{2+} > Fe^{2+} > Fe^{3+} > Li^{+}$. To resolve the ambiguity, we calculated the geometric parameters for all of the optimized structures of isomorphously substituted clusters and an explanation is generated. It is observed that the geometry of the active site is affected with the nature of cation present in the octahedral site substituting aluminum. The variation of the H−O−T angle for each substituted situation is in the order Mg^{2+} (102.78) > Fe^{2+} (102.21) > Fe^{3+} (101.97) > Li^{+} (90.78). The result shows the activity order as predicted from Fukui function is explainable. Magnesium substituted clusters having the highest H−O−T result in the highest activity of −OH hydrogen, so this phenomenon is dependent on the internal structure and configuration. We compared the localized properties in terms of Fukui function and local softness for the octahedral magnesium substituted cluster representing Montmorillonite with tetrahedral aluminum substituted cluster representing Beidellite. The aim is to compare the activity of structural and bridging hydroxyl hydrogen present in the clay structure. The results are shown in Table 3. The results show that for a situation with tetrahedral Al^{3+} substitution the surface hydroxyl is more active than the bridging hydroxyl attached to octahedral aluminum. This is because the layer charge of Beidellite originated from the tetrahedral substitution and not from octahedral substitution. Combing the activities of these two sets of clay clusters, the order of activity in terms of hydroxyl hydrogen (both bridging and structural) is $Al^{3+} > Mg^{2+} > Fe^{2+} > Fe^{3+} > Li^{+}$. Now the results show that the trend observed from global parameters such as global softness and substitution energy is different from the trend obtained from localized parameters. This is justifiable phenomenon and a limitation of localized cluster calculation. Here our aim is to choose a sorbent from the clay structures for sorption of toxic organic molecules. This can be achieved by comparing the activity index present at the local active centers of the interacting molecules, which in another way will result in estimating the nature of interaction between most nucleophilic site of clay structure with the most electrophilic site of dioxins/furans. The specific interaction of the molecule with clay surface will be discussed in the following sections.

Interaction of TCDD and TBDD with Clay Clusters. The labeled model of TCDD is shown in Figure 3a. The bromine substitution is at the same position as the chlorine is in TBDD. The Fukui function (f_x^-) and local atomic softness (s_x^-) for the constituent atoms of the TCDD and TBDD molecules are calculated using the ESP method with DFT, and the results are shown in Table 4. The results show that the most electrophilic site of the TCDD and TBDD molecules is the chlorine/bromine atom attached and that this atom is more active than the oxygen present in the ring. These active centers will interact with the most nucleophilic site of the clay clusters, depending on the values of the Fukui function and local softness values of the interacting species.

Interaction of TCDF and TBDF with Clay Clusters. The labeled model of TCDF is shown in Figure 3b. The bromine substitution is at the same position as the chlorine is in TBDF. The Fukui function (f_x^-) and local atomic softness (s_x^-) for the constituent atoms of the TCDF and TBDF molecules are calculated using the ESP method with DFT, and the results are shown in Table 5. The results show that the most electrophilic site of the TCDD and TBDD molecule is the chlorine/bromine

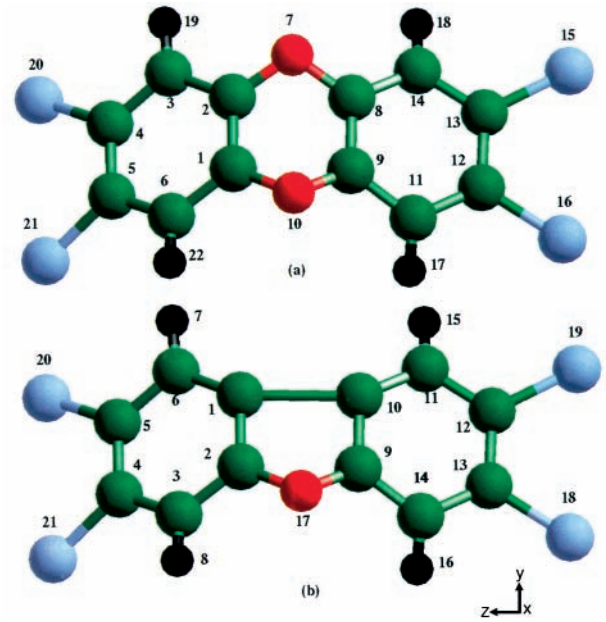

Figure 3. Initial configuration of (a) TCDD and (b) TCDF molecules labeled as shown in Tables 4 and 5. The location of Br in TBDD and TBDF is similar to that of Cl in TCDD and TCDF. The color code is as follows: green (carbon); red (oxygen); black (hydrogen); blue (chlorine).

atom attached and this atom is more active than the oxygen present in the ring. So the electrophilic site of these two molecules may interact with the nucleophilic centers of the clay clusters having closest match of Fukui function and local softness values.

Reactivity Index Scale. The aim of the current study is to rationalize an understanding by which to choose a sorbent material from the dioctahedral smectite family for selective sorption of highly toxic dioxins and furans. We have used two sets of clay clusters to monitor the role of different types of hydroxyl hydrogen present in the clay cluster. It is observed that in terms of global softness values TCDD is the highest and TBDF is the lowest. The order in terms of global softness is as follows: TCDD > TBDD > TBDF > TCDF. The order of global softness of different isomorphously substituted clay clusters is as follows: $Al^{3+} > Li^{+} > Mg^{2+} > Fe^{2+} > Fe^{3+}$.

We present the results of condensed local softness and Fukui functions of the most nucleophilic atom of the cluster models with different isomorphous substitution from the ESP techniques in Table 2 and Table 3. The results show that both in terms of Fukui functions and condensed local softness the hydroxyl hydrogens attached to different octahedral/tetrahedral cations in interacting clay cluster can be arranged in the order $Al^{3+} > Mg^{2+} > Fe^{2+} > Fe^{3+} > Li^{+}$. To monitor the match between the local softness of the electrophilic center of the organic toxic molecules to that of nucleophilic center of the clay clusters we calculated the ratio of s_x^+ and s_x^-. The results are shown in Figure 4. The results show that for all sets of molecules the activity order is $Al^{3+} > Mg^{2+} > Fe^{2+} > Fe^{3+} > Li^{+}$. Though the trend is purely qualitative, certainly it shows that the surface hydroxyl present in Beidellite has higher activity in comparison to the bridging hydroxyl present in substituted clusters of Montmorillonite. The lithium substituted cluster is the worst match. These results, however, tell us that aluminum substituted Beidellite will be the best candidate for sorption of dioxin and furans, even better than the magnesium substituted clusters representing Montmorillonite. To validate the proposed order we need to perform the interaction energy calculation, which

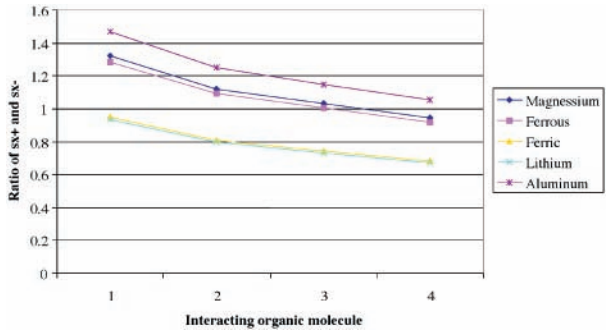

Figure 4. Ratio of local softness for the nucleophilic site to that of the electrophilic site is plotted against each of the interacting organic toxic molecules. The molecules are represented as follows: 1. TCDD, 2. TBDD, 3. TCDF, and 4. TBDF.

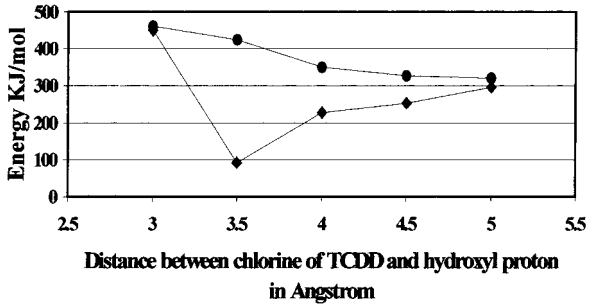

Figure 5. Potential energy curve to study the feasibility of interaction between hydroxyl proton attached with the octahedral center and the chlorine of TCDD in terms of the distance between each other for both Montmorillonite (◆) and Beidellite (●).

is described in the following paragraphs. Prior to that, to locate the minimum energy conformation of the interacting organic species we performed a configuration search using DFT.

Comparison of Activity of Two Types of Hydroxyl Hydrogen Present in Beidellite and Montmorillonite in Terms of the Interacting Species. As we know, the layer charge results from the substitution of tetrahedral/octahedral metal ion present in 2:1 dioctahedral smectite. The octahedral substitution occurs in Montmorillonite type of clay, whereas the tetrahedral substitution occurs for Beidellite types of clay to generate the layer charge. Now both of the clays have structural hydroxyl lying on the surface and hydroxyl hydrogen lying at the octahedral center. From the reactivity index scale it is observed that the structural hydroxyl of Beidellite is more active than hydroxyl hydrogen of Montmorillonite. To find the configuration and orientation of interacting molecules with respect to the clay cluster, we designed the following calculations. In the first case we placed the dioxin molecule TCDD parallel to the clay surface, we fixed the clay cluster, and optimized the TCDD at various distances from the clay framework. We used the magnesium substituted cluster for Montmorillonite because it is the best performer as observed from the reactivity index scale. The stabilization energy with respect to the distance between chlorine of TCDD and hydrogen of hydroxyl hydrogen is plotted in Figure 5. The results show that there exists a sharp minima at a distance of 3.5 Å, whereas for Beidellite there is no such behavior, suggesting that the hydroxyl hydrogen is less active in comparison to that of montmorillonite. The results find support in terms of formation of hydrogen bonding between water and the hydroxyl proton present in Montmorillonite, as mentioned in an IR study.[44] Prost et al.[45] have proposed that in case of smectites, which have their isomorphous substitution in the tetrahedral sheet, water molecules are involved in hydrogen bonding with oxygen atoms

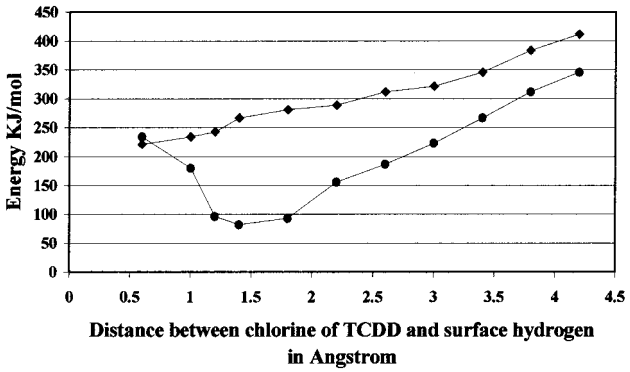

Figure 6. Potential energy curve to study the feasibility of interaction between the surface hydroxyl proton close to the tetrahedral substitution and the chlorine of TCDD in terms of the distance between each other for both Montmorillonite (◆) and Beidellite (●).

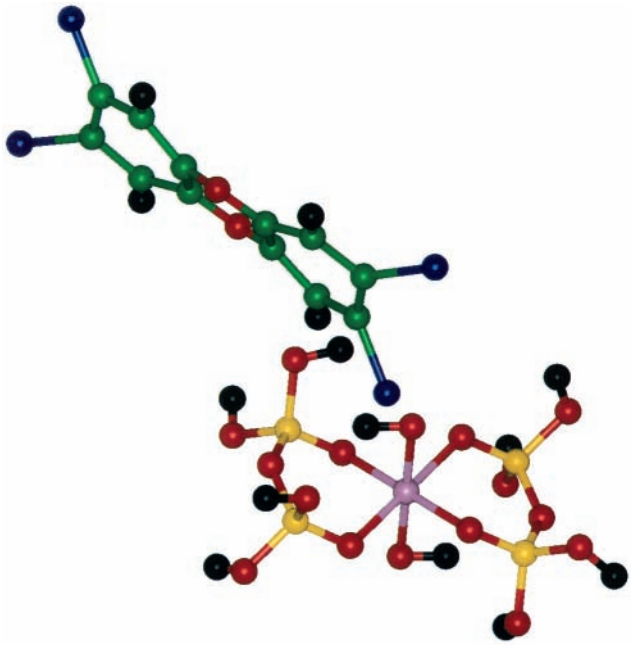

Figure 7. Optimized structure of TCDD molecule during interaction with magnesium substituted Montmorillonite type clay cluster. The color code is red (oxygen); yellow (silicon); violet (octahedral aluminum); black (hydrogen); green (carbon); indigo (chlorine).

belonging to the tetrahedral aluminum replacing tetrahedral silicon. In the second case we aim to monitor the interaction between the surface hydroxyl of clay and the chlorine atom of TCDD. Here we placed the TCDD over the clay surface in a direction so that the surface hydroxyl is directed toward the chlorine of TCDD. The clay cluster is fixed, and the TCDD was optimized at different distances between chlorine of TCDD and the surface hydroxyl hydrogen of clay cluster. The results are shown in Figure 6. The results show that surface interaction is a more feasible process in Beidellite. The distance between the surface hydroxyl hydrogen and chlorine becomes 1.5 Å. This validates the higher activity of Beidellite type of clays over Montmorillonite type of clays. The basic bonding characteristic for the sorption of dioxin type of molecules is the abstraction of chlorine through the formation of HCL, which seems more likely in Beidellite than in Montmorillonite. The optimized configurations of TCDD over Montmorillonite and Beidellite are shown in Figure 7 and Figure 8, respectively.

Interaction of Clay Clusters with TCDD, TBDD, TCDF, and TBDF. The interaction energy calculation was performed

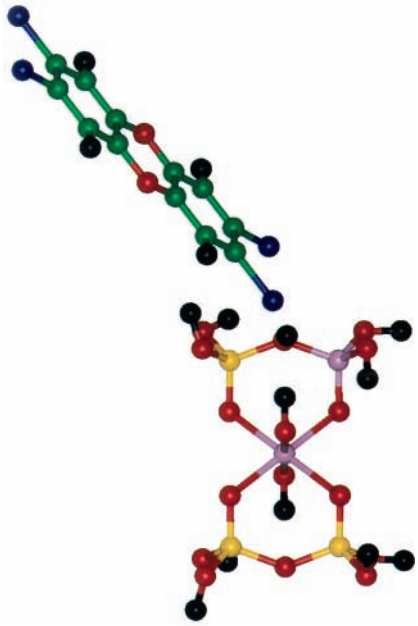

Figure 8. Optimized structure of TCDD molecule during interaction with aluminum substituted Beidellite type clay cluster. The color code is red (oxygen); yellow (silicon); violet (octahedral aluminum); black (hydrogen); green (carbon); indigo (chlorine).

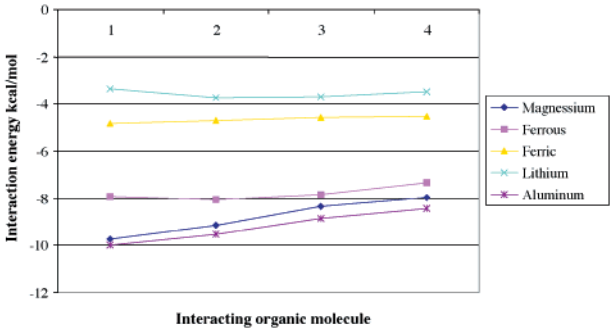

Figure 9. BSSE corrected interaction energy (kcal/mol) is plotted with respect to the interacting organic toxic molecules. The molecules are represented as follows: 1. TCDD, 2. TBDD, 3. TCDF, and 4. TBDF.

using DFT with the BLYP functional. The clay clusters at their respective optimized structures were fixed and the interacting organic molecules are optimized in two different orientations: (1) for Montmorillonite as shown in Figure 7 and (2) for Beidellite as shown in Figure 8. For each case the most electrophilic atom of the interacting organic species (as observed from the reactivity index values) was placed at a distance of 3.5 Å from the hydroxyl hydrogen attached to the octahedral cation of clay cluster acting as the electrophilic center for Montmorillonite type of clay. The distance reduces to 1.5 Å for the clusters representing Beidellite. The results of the interaction energy (BSSE corrected) of the cases are shown in Figure 9. The interaction energy is plotted with respect to the interacting organic species. The interaction energy values fall in the range 2.89 kcal/mol to 9.98 kcal/mol. We will not emphasize the numbers; rather we will analyze the trend. The interaction energy values show the order with respect to the sorption of dioxin and furans. The aluminum substituted Beidellite cluster is the best performer in terms of the interaction energy calculation, and the lithium substituted Montmorillonite type is the worst. The trend is: $Al^{3+} > Mg^{2+} > Fe^{2+} > Fe^{3+} > Li^{+}$. The result matches with the order predicted in terms of the reactivity index values. The adsorption trend for the interacting species is TCDD > TBDD > TCDF > TBDF. The same trend is well observed in terms of the ratio of s_x^+ and s_x^-. Hence these clay materials can selectively adsorb dioxins and furans. This also validates our earlier proposition[30] that the reactivity index scale is nice for unit site interaction, i.e., the interaction of the most nucleophilic site with most electrophilic site. So the postulate proposed for zeolites holds good for clays as well. Hence, from DFT-based local parameters, one can conclusively locate the active site and hence the best material for a particular reaction. This is a novel way to resolve the immense difficulty associated with handling toxic species such as dioxin and will get rid of the tedious and difficult experimentation needed for material designing.

Conclusion

This is the first theoretical study to design a suitable inorganic sorbent material that is economically and environmentally viable for the effective and selective sorption of highly hazardous dioxin and furans. This study also aims to rationalize an understanding between the sorption of organic molecules with clay surfaces with respect to the hydroxyl hydrogen connected to the octahedral/tetrahedral moiety of the framework with different isomorphous substitution at its octahedral layer. The presence of two types of hydroxyl is identified in dioctahedral clays and their roles in their respective activities are also rationalized. Beidellite type clays show viability as a candidate for sorption of dioxin type of molecules over the popular Montmorillonite type. The sorption process is more favorable in Beidellite type of clays. The results show that that the reactivity indices can help to design a new material in terms of its electronic structure. The current methodology can qualitatively locate the active center in a material and the interacting species, which can then be correlated to find a plausible mechanism for a typical reaction. Materials such as dioxin are so toxic that experimentations are very difficult. At the same time the concentration of dioxin in the atmosphere is very low to estimate which needs a solid sorbent for concentration and further decomposition if possible. At the same time our current work involves a wide array of organic toxic pollutants whose preconcentration with clays will be the cheapest solution of the problem, as the natural occurrence of clay in earth is still plenty. The optimized geometry vividly shows that prediction of pseudo bond formation between nucleophilic and electrophilic moieties is possible in the helm of HSAB principle. The optimistic results pave the way for expanding the methodology for other systems as well. Simultaneously the theoretical observation demands experimentation, which is under way.

References and Notes

(1) Bumb, R. R.; Crummett, W. B.; Cutie, S. S.; Gledhill, J. R.; Hummel, R. H.; Kagel, R. O.; Lamparski, L. L.; Luoma, E. V.; Miller, D. L.; Nestrick, T. J.; Shadoff, L. A.; Stehl, R. H.; Woods, J. S. *Science* **1980**, *210*, 385.

(2) Karasek, F. W.; Onuska, F. I. *Anal. Chem.* **1982**, *54*, 309A.

(3) (a) Travis, C. A.; Hattermer-Frey, H. A. *Chemosphere* **1990**, *20*, 729. (b) Streibich, R. C.; Rubey, W. A.; Tirey, D. A.; Dellinger, B. *Chemosphere* **1991**, *23*, 1197.

(4) Kimborough, R. D. *Arch. Environ. Health* **1972**, *25*, 125.

(5) Aitio, A.; Hesso, A.; Luomoto, M.; Rosenberg, C. *Chemosphere* (special issue on chlorinated dioxins and related compounds) **1993**, *27*, 516.

(6) Reddy, V. V.; Patterson, D. G., Jr.; Graiger, G. *Chemosphere* **1989**, *18*, 1.

(7) Makino, M.; Kamiya, M.; Matsushita, H. *Chemosphere* **1992**, *24*, 291.

(8) Koester, C. J.; Hites, R. A. *Chemosphere* **1988**, *17*, 2355.

(9) Cheney, B. V.; Tolly, T. *Int. J. Quantum Chem.* **1979**, *16*, 87.

(10) Schaefer, T.; Sebastian, R. *THEOCHEM* **1990**, *204*, 41.

(11) McKinny, J. D.; Chae, K.; McConell, E. E.; Birnbaum, L. S. *Environ. Health Perspect.* **1985**, *60*, 57.
(12) Fuji, T.; Tanaka, K.; Tokiwa, H.; Soma, Y. *J. Phys. Chem.* **1996**, *100*, 4810.
(13) Jackson, D. R.; Roulier, M. H.; Grotta, H. M.; Rust, S. W.; Warner, J. S. *Chlorinated Dioxins and Dibenzofurans in Perspective*; Rappe, C., Choudary, G., Keith, I. H., Eds.; Lewis Publishers: Chelsea, Michigan, 1986; pp 185−200.
(14) Weber, W. J., Jr.; Voice, T. C.; Pibazari, M.; Hunt, G. E.; Ulanoff, D. M. *Water Res.* **1983**, *10*, 1443.
(15) Karickhoff, S. W.; Brown, D. S.; Scott, T. A. *Water Res.* **1979**, *13*, 241.
(16) Srinivasan, K. R.; Fogler, H. S. *Chlorinated Dioxins and Dibenzofurans in Perspective*; Rappe, C., Choudary, G., Keith, I. H., Eds.; Lewis Publishers: Chelsea, Michigan, 1986; pp 519−530.
(17) Srinivasan, K. R.; Fogler, H. S.; Gulari, E.; Nolan, T.; Schultz, J. S. *Environ. Prog.* **1985**, *4*, 239.
(18) Boyd, S. A.; Mortland, M. M. *Nature* **1985**, *316*, 532.
(19) (a) Chatterjee, A.; Iwasaki, T.; Ebina, T. *J. Phys. Chem. A* **2000**, *104*, 8216 and references therein. (b) Chatterjee, A.; Iwasaki T.; Ebina, T. *Comput. Mater. Sci.* **1999**, *14*, 119.
(20) Pearson, R. G. *J. Am. Chem. Soc.* **1983**, *105*, 7512.
(21) Pearson, R. G. *J. Chem. Educ.* **1987**, *64*, 561.
(22) Parr, R. G.; Yang, W. *J. Am. Chem. Soc.* **1984**, *106*, 4049.
(23) Langenaeker, W.; Demel, K.; Geerlings, P. *J. Mol. Struct. (THEOCHEM)* **1992**, *259*, 317.
(24) Langenaeker, W.; Proft, F. D.; Geerlings, P. *J. Phys. Chem.* **1995**, *99*, 6624.
(25) Langenaeker, W.; Proft, F. D.; Geerlings, P. *J. Phys. Chem. A* **1998**, *102*, 5944.
(26) Chandra, A. K.; Geerlings, P.; Nguyen, M. T. *J. Org. Chem.* **1997**, *62*, 6419.
(27) Chatterjee, A.; Iwasaki, T.; Ebina, T. *J. Phys. Chem. A* **1999**, *103*, 2489 and references therein.
(28) Gazquez, J. L.; Mendez, F. *J. Phys. Chem.* **1994**, *98*, 4591.
(29) Yang, W.; Mortier, M. J. *J. Am. Chem. Soc.* **1986**, *108*, 5708.
(30) Pearson, R. G.; Parr, R. G. *J. Am. Chem. Soc.* **1983**, *105*, 7512.
(31) Kohn, W.; Sham, L. J. *Phys. Rev. A* **1965**, *140*, 1133.
(32) Becke, A. *J. Chem. Phys.* **1988**, *88*, 2547.
(33) Lee, C.; Yang, W.; Parr, R. G. *Phys. Rev. B* **1988**, *37*, 786.
(34) Bock, C. W.; Trachtman, M. *J. Phys. Chem.* **1994**, *98*, 95.
(35) (a) Sim, F.; St-Amant, A.; Papai, I.; Salahub, D. R. *J. Am. Chem. Soc.* **1992**, *114*, 4391. (b) Kim, K.; Jordan, K. D. *J. Phys. Chem.* **1994**, *98*, 10089.
(36) Chandra, A. K.; Nguyen, M. T. *Chem. Phys.* **1998**, *232*, 299.
(37) Boys, S. F.; Bernardi, F. *Mol. Phys.* **1970**, *19*, 553.
(38) Proft, F. D.; Martin, J. M. L.; Geerlings, P. *Chem. Phys. Lett.* **1996**, *250*, 393.
(39) Geerlings, P.; Proft, F. D.; Martin, J. M. L. *Recent Developments in Density Functional Theory; Theoretical and Computational Chemistry 5*; Seminario, S., Ed.; Elsevier: Amsterdam, 1996; pp 773−780.
(40) Chatterjee, A.; Hayashi, H.; Iwasaki, T.; Ebina, T.; Torii, K. *J. Mol. Catal. A* **1998**, *136*, 195.
(41) Chatterjee, A.; Iwasaki, T.; Ebina, T.; Hayashi, H. *J. Mol. Graphics* **1996**, *14*, 302.
(42) Goldschmidt, V. M. *Skr. Nor. Vidensk. Akad. [Kl.], Mat. Naturvidensk. Kl.* 1926.
(43) Arnowitz, S.; Coyne, L.; Lawless, J.; Rishpon, J. *Inorg. Chem.* **1982**, *21*, 3589.
(44) Sposito, G.; Prost, R. *Chem. Rev.* **1982**, *82*, 553.
(45) Prost, R.; Koultit, A.; Benchara, A.; Huard, E. *Clays Miner*. **1998**, *46*, 117.